Biogeosciences Discuss., 8, 549–592, 2011
www.biogeosciences-discuss.net/8/549/2011/
doi:10.5194/bgd-8-549-2011

Biogeosciences Discussions

Modeling biogeochemical processes in sediments from the Rhône River prodelta area (NW Mediterranean Sea)

L. Pastor[1,*], C. Cathalot[2,*], B. Deflandre[1,3], E. Viollier[1], K. Soetaert[4], F. J. R. Meysman[4], C. Ulses[5], E. Metzger[6], and C. Rabouille[2]

[1]Laboratoire de Géochimie des Eaux, UMR 7154, Université Paris Diderot – Paris 7 and IPGP, Batiment Lamarck, Case Postale 7052, 75205 Paris cedex 13, France
[2]Laboratoire des Sciences du Climat et de l'Environnement, CEA-CNRS UMR 1572, Av. de la Terrasse, 91198 Gif sur Yvette, France
[3]UMR 5805 EPOC – OASU, Université Bordeaux 1 – CNRS, Avenue des Facultés, 33405 Talence cedex, France
[4]NIOO-KNAW, Centre for Estuarine and Marine Ecology, Korringaweg 7, 4401 NT Yerseke, The Netherlands
[5]Laboratoire d'Aérologie, CNRS et Université de Toulouse, 14 avenue Edouard Belin, 31400 Toulouse, France
[6]Laboratoire des Bio-Indicateurs Actuels et Fossiles, UPRES EA 2644, UFR Sciences 2 bd Lavoisier, 49045 Angers Cedex 01, France

Discussion Paper | Discussion Paper | Discussion Paper | Discussion Paper |

[7] Laboratoire des Bio-Indicateurs Actuels et fossiles, UPRES EA 2644, UFR Sciences
2 bd Lavoisier, 49045 Angers Cedex 01, France
* These authors contributed equally to this work.

Received: 7 December 2010 – Accepted: 14 December 2010 – Published: 19 January 2011

Correspondence to: L. Pastor (lucie.pastor@eas.gatech.edu)

Published by Copernicus Publications on behalf of the European Geosciences Union.

BGD
8, 549–592, 2011

Biogeochemical processes in the Rhône prodelta sediments

L. Pastor et al.

Abstract

In-situ oxygen microprofiles, sediment organic carbon content and pore-water concentrations of nitrate, ammonium, iron, manganese and sulfides obtained in sediments from the Rhône River prodelta and its adjacent continental shelf were used to constrain a numerical diagenetic model. Results showed that (1) organic matter from the Rhône River is composed of a fraction of fresh material associated to high first-order degradation rate constants (11–33 yr^{-1}), (2) burial efficiency (burial/input ratio) in the Rhône prodelta (within 3 km of the river outlet) can be up to 80%, and decreases to ~20% on the adjacent continental shelf 10–15 km further offshore (3) there is a large contribution of anoxic processes to total mineralization in sediments near the river mouth, certainly due to large inputs of fresh organic material combined with high sedimentation rates, (4) diagenetic by-products originally produced during anoxic organic matter mineralization are almost entirely precipitated (>97%) and buried in the sediment, which leads to (5) a low contribution of the re-oxidation of reduced products to total oxygen consumption. Consequently, total carbon mineralization rates as based on oxygen consumption rates and using Redfield stoichiometry can be largely underestimated in such River Ocean dominated Margins (RiOMar) environments.

1 Introduction

Processes affecting organic matter (OM) in coastal seas sediments are of major importance: OM recycling contributes to the CO_2 balance of the coastal ocean (Borges, 2005; Chen and Borges, 2009) and represents a source of new nutrients to the water column (Rizzo and Christian, 1996; Pratihary et al., 2009) thus contributing to the productivity of the coastal zone (Ingall and Jahnke, 1994; Wollast, 1998). It also influences carbon preservation in marine sediments, especially in River deltas (Aller et al., 1996; Berner and Berner, 1996). The suboxic and anoxic oxidation of OM is of particular interest in these zones since oxygen is consumed rapidly, and thus nitrate, Mn-oxides, Fe-oxides and sulfate are used as terminal electron acceptors (Canfield et al., 1993a). Numerous secondary reactions such as precipitation/dissolution processes (Mucci and Morse, 1984; Canfield and Berner, 1987; Berelson et al., 1990) and redox reactions (Canfield et al., 1993a, b; Deflandre et al., 2002) take place in the sedimentary column, affecting concentration gradients, and thus diffusive fluxes of dissolved components (Berner, 1980). In particular, it is important to estimate the rates and relative importance of the different mineralization pathways when assessing the modification of organic carbon (OC) fate in response to environmental changes (Holligans and Reiners, 1992). These degradation rates can be determined indirectly from the pore-water concentration profiles coupled to diagenetic models (e.g., Boudreau, 1991, 1997; Rabouille and Gaillard, 1991; Dhakar and Burdige, 1996; Soetaert et al., 1996a; Van Cappellen and Wang, 1996; Wang and Van Cappellen, 1996; Berg et al., 2003). These models are based on the 1-D description of the sedimentary column and are mostly applied to environments under steady-state conditions. In this work this approach is utilized to explore a river dominated ocean margins area (RiOMar) where both benthic mineralization and preservation of organic matter are intense. More particularly, these specific systems which undergo very large sedimentation rates (McKee et al., 2004) still require refinement of our understanding of the interplay between mineralization and burial processes.

The Rhône River prodelta and its adjacent continental shelf is an interesting example of these RiOMar systems. Due to the damming of the Nile, the Rhône River becomes the most important river of the Mediterranean Sea both in terms of water and particle discharges (Copin-Montegut, 1993; Pont et al., 2002). Its influence over the continental shelf of the Gulf of Lions has been widely documented (Monaco et al., 1999; De Madron et al., 2000; Sempéré et al., 2000; Lansard et al., 2009). For instance, recent studies highlighted the distribution of organic carbon in the sediments near the Rhone delta and discussed its origin and lability (Tesi et al., 2007; Lansard et al., 2009). Several studies have also emphasized the tight link between the distribution of the Rhône River inputs and the benthic mineralization activity assessed from sediment oxygen

BGD
8, 549–592, 2011

fluxes (Lansard et al., 2009; Cathalot et al., 2010; Pastor et al., 2011). Nevertheless, these studies have focussed on specific aspects of the benthic OC cycle while a quantitative approach with a process model including anoxic diagenesis is needed to fully assess the functioning of the Rhône River prodelta and its adjacent continental shelf.

The present study makes use of a diagenetic model constrained by concentration profiles. It provides a better understanding of the biogeochemical cycles in the close vicinity of the Rhône River outlet concerning (1) the fate of particles imported by the Rhône River (mineralization and burial) on a large time scale, (2) the degradability of organic matter (OM) deposited at the sediment surface and its impact on the mineralization processes, (3) the relative importance of anoxic processes vs. oxic processes and (4) the behaviour of diagenetic products and their contribution in the total oxygen consumption. The latter is important to assess the validity of oxygen microprofiles as a proxy of OC oxidation.

2 Material and methods

2.1 Study area

The Rhône River is 812 km long and presents an annual average water discharge of 1700 $m^3 s^{-1}$ (Pont et al., 2002; Antonelli et al., 2004). Its main channel, Grand Rhône, encompasses 90% of the total river water flux. The Rhône prodelta represents a 30 km^2 area close to the Rhône River mouth (Aloisi et al., 1982; Durrieu de Madron et al., 2000). It is characterized by very high sedimentation rates up to 41 $cm\,yr^{-1}$ and high organic carbon content (1–3%). The sedimentation rates decrease with the distance from the mouth to reach values less than 1 $cm\,yr^{-1}$ on the continental slope (Zuo et al., 1997). The high concentrations of benthic organic carbon in the prodelta reflect the Rhône River inputs i.e. the amount of organic carbon discharge originating from erosion and runoff in the drainage basin (Buscail et al., 1995; Lansard et al., 2005; Pastor et al., 2010). In its adjacent continental shelf (up to 25 km from the river outlet), this influence is less marked and some marine influence is observed (Lansard et al., 2009). The river plume is generally oriented southwestward but eastward currents can occur (up to 18% of the time), thus changing the direction of the plume (Gatti et al., 2006).

2.2 In situ oxygen microprofiling: oxygen flux calculation

Oxygen and resistivity profiles were measured in situ at 200 µm resolution by a benthic microprofiler (Unisense®) equipped with four O_2 microelectrodes and one resistivity sensor. The complete description of oxygen profile acquisition is given by Cathalot et al. (2010). Briefly, dissolved oxygen concentration was measured by oxygen microelectrodes (Unisense®) provided with a built-in reference and an internal guard cathode (Revsbech, 1989). The O_2 microsensors had tip outer diameters of 100 µm, a stirring sensitivity of <1%, a 90% response time <10 s, and less than 2% per hour current drift. A linear calibration for the microelectrodes was used between the bottom water oxygen content estimated by Winkler titration (Grasshoff et al., 1983) and the anoxic zone of the sediment. The classical method which consists of assigning the interface location to a break in the oxygen concentration gradient was performed on the in situ oxygen microprofiles.

Diffusive oxygen uptake (DOU) was calculated from O_2 microprofiles using the 1-D Fick's first law of diffusion, $J=-\phi D\frac{dC}{dz}$, where J is the flux, C is the concentration, ϕ the sediment porosity and D the molecular diffusion coefficient of oxygen at in situ temperature.

2.3 Sampling

Sampling sites were located within 23 km off the Rhône River mouth with water depths ranging between 24 m and 89 m (Table 1). Nine sites were visited during April 2007 (Fig. 1) under moderate discharge conditions (600–1000 $m^3 s^{-1}$) and low wave significant heights (<1 m). Bottom water measurements of temperature, salinity and oxygen concentration were performed on Niskin bottle samples taken 2 m above bottom.

Discussion Paper | Discussion Paper | Discussion Paper | Discussion Paper |
BGD
8, 549–592, 2011
Biogeochemical processes in the Rhône prodelta sediments
L. Pastor et al.
Title Page
Abstract Introduction
Conclusions References
Tables Figures
◀ ▶
Back Close
Full Screen / Esc
Printer-friendly Version
Interactive Discussion

Sediment cores from the 9 sites were collected with an Oktopus multicorer GmbH. Up to eight cores of 10 cm inner diameter were collected at each site with corer penetration depth between 20 and 40 cm. Cores were sampled and maintained at in situ temperature until further analysis. Pore-water and solid phase profiles were sampled on a single core per station: sediments were subsampled under nitrogen atmosphere according to a vertical grid, every 0.5 cm over the 1st cm, every 1 cm over the next 10 cm, and at 2 cm intervals below. Sediments were then transferred into 50 mL polypropylene Falcon™ tubes and centrifuged under N_2 atmosphere. Pore-waters were extracted and immediately acidified (69% suprapur HNO_3^-, Merck) to ~pH 2 or frozen (−20 °C) depending on the analyses. The sediment solid phase was immediately frozen to maintain the anoxic conditions of the sediments.

2.4 Dark core incubations

Sediment incubations were performed in the dark on three undisturbed sediment cores per station kept at in situ temperature. Once totally filled and sealed with a gasproof cap, core tubes were placed in a water bath at in situ bottom temperature (±1 °C). Overlying water into the cores was constantly stirred at about 30 rpm using a Teflon coated magnetic stirring bar attached to the core lid. Magnetic stirrers, centered on the lid of each core, allowed the stirring bars to circulate with the same speed in all the three cores. Every 2–3 h, 50 mL of the overlying water was sampled and replaced with the same volume of filtered bottom water (Hulth et al., 1997). Total fluxes of oxygen, nitrate and ammonium were then calculated from the difference in concentration between samples in each incubation core, corrected for the replacement water. The incubation period and sampling intervals were adjusted so that oxygen concentration in the overlying water never fell below approximately 70% from the original ambient value (Hulth et al., 1997). Incubations typically lasted for 18 h with sampling intervals of 2–3 h.

BGD
8, 549–592, 2011

2.5 Solid phase analyses

Porosity was calculated based on water contents (as assessed by the difference between wet and freeze-dried weight) and assuming a sediment bulk density of $2.65\,g\,cm^{-3}$. Porosity was corrected for the salt content using bottom waters salinities.

Sediment OC contents were assessed on a single core. Corresponding samples were freeze-dried and homogeneously crushed. Precisely weighed subsamples (± 0.001 mg DW) were then analyzed in an automatic CHNS-Thermofisher analyzer, after overnight acidification with 8% H_3PO_4 (within the tin cap) to remove carbonates prior to the determination of organic carbon. Another aliquot was analyzed for sulfur content after addition of vanadium pentoxide. Two certified soils (Soil reference material for NCS determination, thermo; IHSS 1S101F) were used to check the accuracy of the analyses. Precisions were typically within 2%.

Sequential extraction techniques were used to determine the manganese and iron solid phase concentration, and in particular manganese and iron oxides (respectively MnO_x and FeO_x). The most reactive manganese and iron oxide fractions (amorphous oxides) were extracted with an ascorbate reagent (Kostka and Luther, 1994; Anschutz et al., 1998, 2000; Haese et al., 2000). This reagent consisted of a deaerated solution of 50 g of sodium citrate and 50 g of sodium bicarbonate in 1 L of deionized water to which 20 g of ascorbic acid was slowly added to a final pH of 8. About 250 mg of dry sediment was extracted at room temperature with 12.5 mL of this reagent while shaking continuously for 24 h. A second extraction on a separate 250 mg aliquot was carried out with 12.5 mL of 1 N HCl for 24 h to determine acid soluble Mn and Fe (respectively Mn_{HCl} and Fe_{HCl}). The centrifuged solutions were then diluted in 0.2 N HCl and analyzed by flame atomic absorption. The ascorbate reagent extracts selectively amorphous manganese and iron oxides (respectively Mn_{Asc} and Fe_{Asc}) and associated elements (Kostka and Luther, 1994). The reactive phases extracted by 1 N HCl represented the operationally defined fraction that comprises amorphous and crystalline Fe

BGD
8, 549–592, 2011

and Mn oxides, carbonates and hydrous aluminum silicates (Huerta-Diaz and Morse, 1990, 1992). It may not include some iron oxides that are readily converted into sulfides such as goethite and hematite (Raiswellet al., 1994).

2.6 Pore water analyses

Pore water was analyzed for nitrate (Grasshoff et al., 1983), ammonia (Helder, 1989) and sulfate (Tabatabai, 1974) using a Quattro-AXFLOW autoanalyser. The acidified subsample was analyzed for Fe^{2+} and Mn^{2+} by GFAAS using a SOLAAR AAS. Total inorganic carbon (DIC) was measured using a flow injection-conductivity detection system as described in Hall and Aller (1992). Dissolved sulphide ($\sum H_2S$) was determined using the methylene blue method (Cline, 1969).

Oxygen demand units (ODUs), i.e. the amount of oxygen necessary to re-oxidize the reduced products resulting from anaerobic mineralization was calculated using the concentration of dissolved iron, manganese and H_2S using the following formula:

$$[\mathrm{ODU}]=\frac{1}{2}[\mathrm{Mn}^{2+}]+\frac{1}{4}[\mathrm{Fe}^{2+}]+2[\mathrm{S}^{2-}]$$

according to the diagenetic equations and the associated stoechiometry (Berner, 1989; Canfield et al., 1993b; Soetaert et al., 1996a), where S^{2-} stands for ΣH_2S.

2.7 Diagenetic modeling

A steady state version of a numerical diagenetic model, OMEXDIA (Soetaert et al., 1996a), as implemented in the open source software R (Soetaert and Herman, 2009), was used and model output was fitted to the measured profiles of oxygen, nitrate, ammonium, ODUs and OC to estimate the rates of total carbon oxidation, the relative contribution of the major pathways of organic matter mineralization (aerobic, anaerobic and denitrification) and oxygen utilization.

Briefly, OMEXDIA is a numerical nonlinear coupled model based on the 1-dimensional diagenetic equations (Boudreau, 1997; Berner, 1980). In this model,

BGD
8, 549–592, 2011

solutes are transported by molecular diffusion, whereas solid phase compounds are transported by advection, compaction and bioturbation. The model describes aerobic carbon mineralization, nitrification and denitrification and combines remaining anaerobic mineralization processes. Solid phase organic carbon is modeled as 2 fractions with different reactivities (and thus different first order mineralization rates) and C/N ratios corresponding to a labile and a more refractory organic matter. The decomposition kinetics are first-order and controlled thus by two rate constants, corresponding to these two types of organic matter. Model output generates steady state profiles of oxygen, nitrate, ammonium, ODUs and OC.

Oxygen, nitrate, ammonium and sediment organic carbon profiles were fitted using an automatic fitting procedure provided by the R package FME (K. Soetaert). Based on previous extensive Monte-Carlo sensitivity analyses (Soetaert et al., 1996a, 1998), the main tuned parameters for this study are (1) the total flux of degradable organic carbon deposited at the surface (Fdeg), (2) its partitioning over a fast and a slow degraded fraction (Pfast), (3) their relative first order degradation constant (respectively Rfast and Rslow), (4) the asymptotic organic carbon content (OC burial), (5) the nitrification rate constant (Rnit) and (6) the burial fraction of reduced species (ODUdepo). For each station, after collinearity among parameters has been checked, a selected set of parameters was then tuned to fit the concentration profiles and fluxes data. A good fit was achieved by minimizing the model cost function which quantifies the discrepancy between observed data and modelled values. High collinearities were found between Fdeg, and both rnit and pFast: rnit was then adjusted regarding to literature and pFast adjusted manually.

Part of the reduced substances produced during the mineralization of organic matter (here expressed as ODUs) are permanently lost from the system (e.g. by precipitation of FeS and pyrite (Berner, 1977) and manganese carbonate (Pedersen and Price, 1982) below the bioturbation zone. The ODUdepo parameter was then used to account for the disappearance of a certain amount of ODUs out of the system (ODUdepo).

Bioturbation coefficients, modeled as a local transport process, were adjusted in accordance to literature (Zuo et al., 1991; Radakovitch et al., 1999) and Sediment Profile Imagery (SPI) data performed during the same cruise. Sedimentation rates were obtained from literature (Zuo et al., 1997; Charmasson et al., 1998, Radakovitch et al., 1999; Miralles et al., 2005). They ranged from 10 cm yr^{-1} close to the mouth (station A) to 0.1 cm yr^{-1} in stations F and J. The mixed layer was averaged to 13 cm as indicated by the SPI data as developed by Rhoads and Cande (1971) (M. Desmalades, personal communication, 2007). C/N values were averaged to 7.1 for the fast fraction and 14.3 for the slow fraction. Diffusivity in water was calculated according to Boudreau (1986) and corrected for salinity, temperature and pressure using the marelac package in R (Soetaert, Petzoldt and Meysman, 2010). The bulk sediment diffusion coefficient of solutes was calculated from Rasmussen and Jorgensen (1992) as $Ds = \frac{D_0}{(1+3(1-\phi))}$ where ϕ is the sediment porosity and D_0 is the diffusion coefficient in water as calculated above. All bottom water conditions (temperature, salinity, dissolved elements concentrations) were measured during the sampling cruise.

3 Results

3.1 Bottom water properties

Bottom water temperature and salinity were homogeneous among all sites ranging respectively between 14.2 and 14.9 °C, and 37.6 and 38.0. Bottom water was well-oxygenated with oxygen saturation between 92 and 100%.

3.2 Pore-water and solid phase composition

Pore-water profiles of measured oxygen, nitrate, ammonium, dissolved manganese and iron, sulfate, DIC, and solid phase profiles of particulate manganese and iron for four stations are shown in Fig. 2. Stations A and B are located near the river mouth,

BGD
8, 549–592, 2011

Biogeochemical processes in the Rhône prodelta sediments

L. Pastor et al.

while station F is 23 km southwestward and station J is 10.7 km southeastward (Fig. 1). The oxygen penetration depths ranged from 1.4 mm at station A to 9.7 mm at station F. In all cores, a peak of nitrate in the oxic zone was observed from 21 µM in site F to 7 µM in site B (Fig. 2). Below the oxic layer, nitrate was then rapidly consumed as indicated by a rapid decrease in nitrate.

Except at station A where the deposition dynamics are highly variable, a decrease in MnO_x and FeO_x was observed concomitantly with an increase in Mn^{2+} and Fe^{2+}. Dissolved manganese and iron concentrations in site A were up to 170 µM and 760 µM, respectively. These concentrations decreased with depth and distance from the mouth to reach an average asymptotic value of ca. 25 µM of Mn^{2+} and 100 µM of Fe^{2+} in site F. Similarly, ammonium and DIC concentrations were extremely high at station A (~3500 µM and ~25 mM, respectively) and decreased with depth and distance from the mouth (<300 µM for NH_4^+ and <5 mM for DIC, at the stations furthest from the mouth). In this area, the stock of Mn_{Asc} and Fe_{Asc} remained available in depth, between 1 and 4 µmol g^{-1} for Mn_{Asc} and between 20 and 100 µmol g^{-1} for Fe_{Asc}.

Sulfate reduction is clearly observable in stations A and B (Fig. 2), and to a lesser extent in station K, N, and C (data not shown) as indicated by a reduction in sulfate concentrations at depth in the sediment. This decrease was not observed at the other stations, nevertheless high concentrations of FeO_x could have also promoted a rapid reoxidation of sulfide (produced by sulfate reduction) to sulfate. Despite the reduction of sulfate, porewater sulfide as measured using colorimetry or microelectrode showed almost no detectable concentration in the micromolar range; down to a depth of 30 cm (data not shown).

3.3 Constraining the model with experimental data

The OMEXDIA model was first applied to represent steady state conditions in low organic flux sediments. It has nevertheless already been used successfully in more productive systems as an eutrophic shallow lagoon in the Mediterranean sea area (Dedieu et al., 2007) and in the Iberian margin (Epping et al., 2002).

BGD
8, 549–592, 2011

For all sites of the present study, satisfactory fits were generally obtained (Fig. 3a, b). The 10 first cm were fitted with highest priority because some non-steady state features may occur at a greater depth (e.g. ammonium profiles, Fig. 2). Measured OC profiles did not exhibit an asymptotic shape at all stations and consequently, an accurate fit was not always possible for this variable. Values of the fitted parameters for the nine stations are given in Table 2.

3.3.1 Organic carbon deposition and reactivity

Deposition fluxes of degradable organic carbon and total organic carbon (as defined by degradable OC+buried OC), obtained from modeling gradually decline offshore along with a decrease in burial efficiency (Fig. 4). Degradable organic carbon fluxes can be up to 657 $\mathrm{g\,C\,m^{-2}\,yr^{-1}}$ when the accumulation rate reaches 10 $\mathrm{cm\,yr^{-1}}$ at station A, this value decreasing to 32 $\mathrm{g\,C\,m^{-2}\,yr^{-1}}$ when the accumulation rate is 0.1 $\mathrm{cm\,yr^{-1}}$ (station F). The flux of OC buried in the prodelta area (i.e. stations A and B) accounts for up to 80% of the total OC flux, this value decreasing offshore to ~20% in stations F and J.

The first-order degradation constants are lower in station A (11 $\mathrm{yr^{-1}}$) than in the other stations (33 $\mathrm{yr^{-1}}$) for the most reactive fraction (Rfast, Table 2). This pattern was not observed for the less reactive fraction (Rslow, Table 2), with no clear spatial pattern and values between 0.21 $\mathrm{yr^{-1}}$ and 0.37 $\mathrm{yr^{-1}}$ spread among the stations. The proportion of the most labile fraction ranged between 50% and 94% (Table 2).

3.3.2 Comparison between model outputs and an independent set of data

To validate the model, the diffusive fluxes of oxygen, nitrate and ammonium calculated from the model were compared to the benthic fluxes measured in dark core incubations during the same cruise. Both type of fluxes could be reasonably compared as TOU/DOU ratios were generally close to 1 (except for stations F, I and J where the ratios are between 1.3 and 1.8, Lansard et al., 2009; Pastor et al., 2011). Results of this comparison are given in Table 1. Oxygen fluxes calculated from the model show a reasonable agreement with experimental data, showing a decrease with distance from the mouth as previously observed (Cathalot et al., 2010; Lansard et al., 2009). As expected from higher TOU/DOU ratios, DOU estimated from the model at stations F, I, and J are lower than TOU measured by core incubations. The ammonium release calculated from the model is also in fair agreement with the core incubations data, whereas nitrate release is slightly overestimated. This overestimation in nitrate release could be due to (1) the coarse resolution of sampling and/or (2), a contamination with oxygen prior to analysis. Nevertheless, as samples were immediately frozen to avoid such bias, this was probably mainly due to the coarse resolution.

3.4 Major model outputs

Oxic OC mineralization rates ranged from 15.7 mmol C m^{-2} d^{-1} at station B to 4.9 mmol C m^{-2} d^{-1} at station F (Table 3). It represents between 8% and 67% of the total OC mineralization rates. As expected, the relative proportion of oxic mineralization to total OC mineralization increased with water depth and distance from the mouth (Fig. 5).

Denitrification rates were higher in the vicinity of the river outlet (station A) with a rate of 4.0 mmol C m^{-2} d^{-1} (Table 3). Further offshore in the continental shelf, these rates decreased to ~0.5 mmol C m^{-2} d^{-1} at stations J and F. Relatively to total OC oxidation rates, the denitrification process remains of little importance with percentages between 2% and 5%. Station A exhibited the highest values of nitrification with 7.1 mmol N m^{-2} d^{-1}, while stations offshore exhibited lower values down to 0.4 mmol N m^{-2} d^{-1}.

Anoxic OC mineralization rates (i.e. the sum of remaining processes: MnO_x, FeO_x and sulfate reduction) showed the same trend as the oxic OC mineralization rates with higher values at station A of 134.0 mmol C m^{-2} d^{-1}, values decreasing to 2.0 mmol C m^{-2} d^{-1} at station F. Figure 5 indicates that the relative part of anoxic and oxic mineralization roughly mirror one another. The relative contribution of anoxic mineralization processes was 89% in the prodelta at station A, this percentage decreased rapidly to a homogeneous steady value around 30–40% in the adjacent continental shelf and down to 27% at station F (Fig. 5). In addition, to fit our Fe^{2+}, Mn^{2+} and ΣH_2S data, high precipitation rates of reduced species were found. The ODUdepo term was then tuned at 99.5% in station A (Table 2) to allow for the disappearance of ODUs. For all sites, this precipitation term ranged between 97.0 and 99.5% (Table 2).

Oxygen was preferentially used for oxic mineralization with a high contribution ranging between 62 and 93% (Table 3). The remaining fraction was used for nitrification (6–37%) and for the re-oxidation of reduced products (1–3%).

4 Discussion

4.1 Organic carbon reactivity

The degradable organic carbon deposited at the sediment surface is composed of a range of OM reactivities (Wakeham et al., 1997). This is represented in the OMEXDIA model by two distinct fractions: a labile fraction and an intermediate reactivity fraction (Soetaert et al., 1996a). These two fractions are represented by a first-order degradation constant which is characteristic of their reactivity. The values obtained in this study (11–33 yr^{-1} and 0.21–0.37 yr^{-1}) were comparable to those of 18 yr^{-1} and 1.1 yr^{-1} (normalized to a temperature of 15 °C using a Q_{10} of 2) reported in Westrich and Berner (1984) from incubation experiments of fresh planktonic material. While the labile fraction of OM has a degradation constant close to fresh planktonic material, the first-order degradation constants for the less reactive material could correspond to resuspended organic matter which could explain the low degradation constant observed (Berner, 1980; Hargrave and Phillips, 1989; Herman et al., 2001). Measurements of biomass accumulation showed very low Chl-*a* levels in the water column (estimated by low fluorescence levels in CTD profiles – J. J. Naudin, personal communication, 2008) during our sampling cruises in the studied area (April 2007, September 2007, June 2008, December 2008) and during other pelagic cruises (May 2008, May 2009). Furthermore,

BGD
8, 549–592, 2011

prodelta sediments were mainly composed of terrigenous OM as evidenced by their $\delta^{13}C$ values of −27‰ (Lansard et al., 2009). This fast decaying fraction most likely represents reactive material of whether riverine or marine phytoplanktonic origin, not assessable with classical bulk measurements as previously described by Pastor et al. (2011).

The two fractions of OM here are then related to the dilution of the Rhône River material (Tesi et al., 2007; Lansard et al., 2009). OM in stations A and B, located in the prodelta, is a mixture of fine and coarse continental material rich in sedimentary organics. These stations present $\delta^{13}C$ depleted values characteristic of terrestrial inputs together with an apparent labile fraction of OM. Further offshore, OM is composed of aged resuspended particles which underwent many deposition/degradation/remobilization cycles and were characterized by lower OC, "heavier" isotopic composition and the absence of lignin (Cathalot et al., 2011).

4.2 Mineralization processes

The highest values of degradable fluxes of organic carbon (Table 2) were found at stations located in the prodelta. This reflects the spatial distribution of OC oxidation processes from modeling (Fig. 5). Our high OC deposition fluxes were higher than the previous estimation of 178 $g\,C\,m^{-2}\,yr^{-1}$ for POC deposition in the whole prodelta reported by Durrieu de Madron et al. (2000). This difference is most likely related to the surface area of the zone studied: our station A was directly located within the prodelta characterized by high sedimentation rates (up to 41 $cm\,yr^{-1}$). Durrieu de Madron et al. (2000) based their calculation on a wider area including more distal stations (our stations B, N, and K) where the slope gradient (and consequently the sedimentation rates gradient) is maximal. The high OC deposition fluxes observed within the prodelta are most likely responsible for the high mineralization rates in this area. Oxygen is thus rapidly consumed within the sediments and anoxic processes become the dominant processes (Fig. 5).

BGD
8, 549–592, 2011

Biogeochemical processes in the Rhône prodelta sediments

L. Pastor et al.

At stations located further on the adjacent continental shelf, values of 30–100 $g\,C\,m^{-2}\,yr^{-1}$ (Table 2) were close to the ones reported in Canfield (1989), who found carbon oxidation rates between ca. 20 $g\,C\,m^{-2}\,yr^{-1}$ and 110 $g\,C\,m^{-2}\,yr^{-1}$ for a similar accumulation rate of 0.1 $cm\,yr^{-1}$. Then, as the distance from the river outlet increases, mineralization rates become lower (Table 3), oxygen penetration depths increase and a progressive dominance of oxic processes takes place (Fig. 5).

This decrease of mineralization rates showed the same pattern as the variation of sedimentation rate as previously observed in other studies (i.e., Canfield, 1989; Tromp et al., 1995). The burial of organic carbon within the prodelta is very high and represents up to 80% of the total OC flux, this value decreased offshore to ca. 20% in stations F and J. For instance, Henrichs and Reeburgh (1987) reported a carbon burial efficiency of up to 80% for a sedimentation rate of 10 $cm\,yr^{-1}$, and ca. 5–20% for a sedimentation rate of 0.1 $cm\,yr^{-1}$.

In order to better assess the controls of benthic OC degradation, we plotted the relative contribution of anoxic processes in OC mineralization as a function of the logarithm of total OC deposition flux of various sediment systems (Fig. 6). There is a significant correlation (n=35, r=0.74, p<0.0001) between the percentage of anoxic mineralization and the logarithm of total OC deposition flux, the highest anaerobic contribution to OC mineralization occurring in regions with the highest POC rain. This is also visible in our sulfate profiles; the most significant consumption (and likely the highest sulfate reduction rates) occurred in stations with maximal accumulation rate. Hargrave et al. (2008) also evidenced an enhancement of microbial sulfate reduction under conditions of high organic matter sedimentation and the progressive formation of suboxic–anoxic conditions. Hebce, our results suggest that the amount of POC vertically exported and reaching the coastal seafloor directly controls the anaerobic mineralization activity and carbon preservation of oceanic sediments (Henrichs and Reeburgh, 1987; Canfield, 1994). The control of OC mineralization by POC rain provides then a critical positive relationship between the burial of reduced materials in sediments and the OC inputs in ocean margins.

BGD
8, 549–592, 2011

4.3 Behaviour of reduced products

Our modeling results clearly show that anoxic mineralization processes play a major role in the Rhône River prodelta, providing crucial information about the OC cycle in this coastal area. Nevertheless, the OMEXDIA model considers all anoxic mineralization processes as a single process leading to the ultimate release of ODUs. Accordingly, the model does not give any insights on the reaction pathways of anaerobic oxidation, nor on the benthic biogeochemical cycles of the elements involved. For instance, at some stations and within the limited coring depth (A and B, and to a lower extent, K, N and C), significant sulfate reduction is most likely to occur as indicated by a significant decrease in sulfate concentration in the lower sedimentary column (Fig. 2). Then, for instance at station B, with no precipitation (pdepo=0), the model generated a production of $5\,\mathrm{mmol\,m^{-2}\,d^{-1}}$ of ODU, whereas the SO_4^{2-} profile allowed the calculation using the PROFILE software program (Berg et al., 1998) of a production of $10\,\mathrm{mmol\,m^{-2}\,d^{-1}}$ of ODU expressed as ΣH_2S. These two numbers are within the same order of magnitude and confirm that sulfate reduction is a major process at station B. The feature is slightly different at station A, where the model generated a production of $67\,\mathrm{mmol\,m^{-2}\,d^{-1}}$ of ODU, versus $20\,\mathrm{mmol\,m^{-2}\,d^{-1}}$ of ODU expressed as ΣH_2S. This overestimation could be due to other mineralization processes not included in the model. For instance, Garcia-Garcia et al. (2006) showed evidence for high rates of methanogenesis within the Rhône prodelta area after the rapid deposition of a thick layer of new sediment. As no measurements of CH_4 were assessed during our study, this hypothesis cannot be confirmed, but is nevertheless not excluded. This part of the discussion will then principally be based on the sulfate reduction process.

Since we observed sulfate reduction but no sulfide accumulation, especially near the river outlet, it is likely that sulfide is being removed from pore water through reactions within the anoxic zone, such as FeS precipitation (Berner, 1977; Westrich and Berner, 1984).

BGD
8, 549–592, 2011

The large magnitude of the ODUdepo term indicates a substantial precipitation of reduced species (>99% at station A), supporting this sulfide precipitation hypothesis. Although such precipitation rates are in the upper range of reported literature data (Chanton et al., 1987; Jorgensen et al., 1990), this "output" term of the model is supported by our data. Indeed, the ODUdepo term can be substantiated by the observed C/N ratios ($\Delta DIC/\Delta NH_4^+$) in pore-water at all the stations. The general equation of oxidation of organic matter producing ODUs in Soetaert et al. (1996a) is expressed as:

$$(CH_2O)_x(NH_3)_y(H_3PO_4) + 1 \text{ oxidant} \rightarrow xCO_2 + yNH_3 + H_3PO_4 + x\text{ODU} + xH_2O$$

Then, the ODU/NH_4^+ ratio in the model reflects the C/N ratio of the degraded organic matter. The C/N of the fast fraction is 7.1 and the C/N of the slow fraction is 14.3. According to their relative proportion (Pfast, 1-Pfast, Table 2), it is then possible to calculate the average C/N ratio of the degradable fraction. Therefore, the slope of the plot of measured ODU (Fe^{2+}, Mn^{2+} and H_2S) against NH_4^+, corrected for diffusion coefficients, gives the C/N ratio in pore-water at each station. The difference between the theoretical C/N ratios without any precipitation in the system from modeling and C/N ratios from measured data gives the proportion of ODU which is precipitated. In station A for instance, the estimated C/N ratio from pore-water is 0.09 vs. 7.82 for the degradable OM (modeling). This means that ~99% of the produced ODUs are missing from the solute phase. Therefore, both our data and modeling results suggest an intense precipitation of reduced species, and most likely an important recombination of the sulfides produced through sulfate reduction.

To estimate the possible limitations of FeS formation, the relative amounts of organic carbon, sedimentary sulfur and iron were plotted in a ternary diagram (Fig. 7; Littke et al., 1991; Lückge et al., 1999). The area below the line reflects iron-limiting conditions whereas, above, pyrite formation can be limited by the availability of sulfate or organic matter. All sediments of the Rhône prodelta area fall above this line indicating that pyrite formation is not iron-limited. Regarding the high amounts of organic carbon in the system and the high sulfate availability in the water column, it is likely that a large quantity of reducible iron limits the occurrence of sulfide-rich porewaters in the Rhône River prodelta sediments. Another efficient reaction pathway for the disappearance of H_2S is manganese or/and iron reduction coupled to partial sulfide oxidation. This process could explain the residual high concentration of Fe^{2+} at depth (Fig. 2) and the very low concentration of ΣH_2S. Our results clearly show that neither Fe^{2+} nor particulate iron are limiting. In addition, iron monosulfide (FeS) and Pyrite (FeS_2) generally represent the major part of reduced inorganic sulfur pools in marine sediments (Berner, 1984; King et al., 1985; Thamdrup et al., 1994).

The retention of freshly produced sulfide varies from one system to another, 10% to 77% being buried in coastal marine sediments (Chanton et al., 1987; Jorgensen et al., 1990). In the case of the highly reduced sediments of the Rhône River prodelta, this retention is thus likely to be very efficient with values higher than 77%. Hedges and Keil (1995) already pointed out that the introduction of greater amounts of labile marine OM could drive the redox environments of deltaic and slope sediments on to sulfate reduction, halting then the iron and manganese-based degradation when these metals are precipitated as insoluble, reduced sulfides. Our results suggest that the terrestrial OM delivered by the Rhône River, constituted of a reactive fraction, also pushes the diagenetic system towards major reduced products burial. Under some depositional/diagenetic regimes, coastal sediments have been evidenced to have a reactive sulphur fraction without significant net addition to this sulphur pool, evidencing important precipitation of reduced sulfides (see Bottrell et al., 2009 and references therein). In addition, the sudden burial by several centimeter of flood sediments is likely to play a major role on anoxic mineralization processes in prodelta sediments and the preservation of reduced compounds (Thamdrup and Dalsgaard, 2000; Quintana et al., 2007). The quality and quantity of river discharge rates (in terms of nutrients, OM, and metal oxides) might therefore predispose the deltaic regions toward different redox regimes, and consequently toward contrasting carbon preservation and reduced species burial efficiencies. Deltaic areas could thus be major centers for burial of reduced diagenetic products, in addition to being major deposit centers for OM (Hedges and Keil,

BGD
8, 549–592, 2011

1995). More investigation is needed to determine the quantitative importance of such processes. Indeed, incorporating such significant storage of reduced species in deltaic areas could have an impact on models of global Fe-S-C cycling. In a further step, the use of a more detailed model of early diagenesis (e.g. the one described in Berg et al., 2003) would allow a better constrain of these anoxic processes.

This intense cycling and removal of reduced substances explains the small amount of oxygen used to re-oxidize reduced products (Table 3). Between 62 and 93% of the total O_2 consumption were used directly for the oxidation of organic carbon (Table 3), the rest was used for the re-oxidation of reduced products and nitrification. An interesting feature of this RiOMar system is the low fraction of oxygen flux associated to the re-oxidation of reduced chemical species such as Fe^{2+}, Mn^{2+} or sulfide (1–3%). Because more than 97% of the ODU originally produced are precipitated at depth as indicated by the ODUdepo term (Table 2), the resulting flux toward the oxic layer is consequently very low. In other studies, the relative contribution of the O_2 uptake by the sediment for the re-oxidation of reduced products is generally higher. Kasih et al. (2009) showed that 47% of the total O_2 consumption was directly used in the OM mineralization, 19% for nitrification and 34% for the re-oxidation of reduced products in the Ago Bay sediments (Japan). Berg et al. (2003) reported an O_2 contribution of 40% for OM mineralization, 12% for nitrification and 48% for re-oxidation of reduced products in arctic marine sediment. A large difference in ammonium concentrations and mineralization rates exists between these studies and the present one. While NH_4^+ concentrations at depth are below 100 µM in Kasih et al. (2009) and below 80 µM in Berg et al. (2003), they can be up to ~3500 µM in station A and remain below 250 µM only at the far station (station F). Similarly, the DIC concentration is also very high with up to ~25 mM at station A. Thus the amount of ODU present in the porewater of our sediments should be much higher. Nevertheless, pore-water data did not show such high concentrations either by porewater extraction or micro-electrode studies (Figs. 2 and 3). As previously mentioned, these high concentrations of ODU were most likely recombined in the system in secondary reactions, and as a consequence were removed

BGD
8, 549–592, 2011

from the porewaters by precipitation of solid phases, as previously discussed.

Our results highlight that oxygen consumption rates in the Rhône River system are mainly related to aerobic mineralization. They do not represent the anoxic mineralization via the re-oxidation of reduced products. This is also shown to be clear by the smooth gradual decrease of oxygen towards 0; if important oxygen consumption would take place at the oxic-anoxic interface, oxygen would disappear much more drastically there – Fig. 3). This leads to a major conclusion concerning the use of dissolved oxygen fluxes to estimate total carbon mineralization rates. Table 4 shows the model output versus the calculated carbon mineralization rates using in situ dissolved oxygen fluxes and Redfield ratio ($O_2/C=138/106$). At station A, the difference is maximal with a carbon mineralization rate of $657\,g\,C\,m^{-2}\,yr^{-1}$ derived from modelling versus only $72\,g\,C\,m^{-2}\,yr^{-1}$ as derived from oxygen profiles, leading to an underestimation of around 89% at this site. This difference is of course lower when anoxic processes and removal of ODU are less important, with an underestimation of around 44% at station F. Thus, in the Rhône River prodelta where precipitation of reduced products are linked to anoxic processes which display very large rates in the sediment column, oxygen is uniquely used for oxic mineralization and nitrification (Table 3). Therefore, the use of dissolved oxygen fluxes as a proxy for carbon mineralization should be used with caution in other RiOMar systems and coastal areas with similar sediment biogeochemistry.

5 Concluding remarks

Mineralization processes that occur in the Rhône prodelta and its adjacent continental shelf are mainly driven by the OM inputs. Our results evidence a close relationship between OM inputs and anaerobic mineralization processes. These inputs, mainly terrestrial, originate from the Rhône River and are composed of a significant fraction of reactive material with degradation constants close to fresh phytoplankton. High deposition of more labile material close to the river is responsible for a rapid consumption of oxygen and an intense OM degradation, mainly driven by anoxic processes. In the

BGD
8, 549–592, 2011

adjacent continental shelf, this predominance of anoxic processes decreases together with the decrease in organic carbon deposition, accumulation rates, and the increase of oxygen exposure time. Our modeling results suggest a major contribution of precipitation processes in the Rhône River prodelta sediments. Sulfate reduction in the river outlet is most likely to be the main anoxic process (although methanogenesis is not excluded) and retention of produced sulfide appears to be very efficient with more than 97% of produced reduced species disappearing from the pore water. This could be associated with (1) the precipitation of FeS or/and FeS_2 and (2) secondary reactions, for instance the re-oxidation of sulfide by Fe-oxides or Mn-oxides. This intense cycling reduces the diffusion of reduced species to the oxic zone, thus limiting the contribution of oxygen flux in the re-oxidation of these products. More insight is however needed on the reaction pathways occurring in this area to better define the metal cycling as well as the contribution of the Mn and Fe reduction processes. Our study clearly highlights the importance of secondary precipitation reactions in RiOMar systems. Our estimations for the Rhône River system draw attention to the need to assess and quantify the burial of precipitated reduced species, especially when trying to assess some sedimentary C budgets in these highly reactive areas.

Acknowledgements. We would like to thank the captain and crew of the R. V. *Tethys II* (CNRS-INSU) and the entire scientific crew of the CHACCRA-RiOMar.Fr cruises for their technical assistance during sample collection. We also thank Bruno Blombled, Amaury Gaillard, Laure Sandoval, Hassiba Lazar for analytic assistance and Pascal Lecroart for modeling assistance. The modeling was performed after two short stays (1 week) by the two first authors at NIOO-CEME. This work was performed jointly by LGE and LSCE during the Ph.D thesis advised by E. Viollier and B. Deflandre for Lucie Pastor and C. Rabouille for Cécile Cathalot. This work was funded by the French national ANR program CHACCRA (contract number ANR-VULN-06-001-01) and the French INSU-EC2CO program RiOMar.fr. It is the IPGP contribution #0000.

BGD

8, 549–592, 2011

The publication of this article is financed by CNRS-INSU.

References

Aller, R. C., Blair, N. E., Xia, Q., Rude, P. D.: Remineralization rates, recycling, and storage of carbon in Amazon shelf sediments, Cont. Shelf Res., 16, 753–786, 1996.

Aloisi, J. C., Cambon, J. P., Carbonne, J., Cauwet, G., Millot, C., Monaco, A., and Pauc, H.: Origin and role of the bottom nepheloid layer in the tranfer of particles into the marine environment – application to the gulf of lions, Oceanol. Acta, 5, 481–491, 1982.

Anschutz, P., Zhong, S. J., Sundby, B., Mucci, A., and Gobeil, C.: Burial efficiency of phosphorus and the geochemistry of iron in continental margin sediments, Limnol. Oceanogr., 43, 53–64, 1998.

Anschutz, P., Sundby, B., Lefrancois, L., Luther, G. W., and Mucci, A.: Interactions between metal oxides and species of nitrogen and iodine in bioturbated marine sediments, Geochim. Cosmochim. Acta, 64, 2751–2763, 2000.

Antonelli, C., Provansal, M., and Vella, C.: Recent morphological channel changes in a deltaic environment. The case of the Rhône River, France, Geomorphology, 57, 385–402, 2004.

Berelson, W. M., Hammond, D. E., and Cutter, G. A.: In situ measurements of calcium carbonate dissolution rates in deep-sea sediments, Geochim. Cosmochim. Acta, 54, 3013–3020, 1990.

Berg, P., Risgaard-Petersen, N., and Rysgaard, S.: Interpretation of measured concentration profiles in sediment pore water, Limnol. Oceanogr., 43(7), 1500–1510, 1998.

Berg, P., Rysgaard, S., and Thamdrup, B.: Dynamic, modeling of early diagenesis and nutrient cycling. A case study in an arctic marine sediment, Am. J. Sci., 303, 905–955, 2003.

Berner, R. A.: Stoichiometric models for nutrient regeneration in anoxic sediments, Limnol. Oceanogr. 22, 781–786, 1977.

Berner, R. A.: Early Diagenesis: A Theoretical Approach. Princeton Series in Geochemistry, edited by: Princeton, N. J., Princeton University Press, Princeton, 241 pp., 1980.
Berner, R. A.: Sedimentary pyrite formation: An update, Geochim. Cosmochim. Ac., 48(4), 605–615, 1984.
Berner, R. A.: Biogeochemical cycles of carbon and sulfur and their effect on atmospheric oxygen over phanerozoic time, Global Planet. Change, 75, 97–122, 1989.
Berner, E. K. and Berner, R. A.: Global environments: Water, Air and Geochemical cycles, Prentice-Hall: Upper Saddle River, NJ, 1996.
Boudreau, B. P.: Modeling the sulfide-oxygen reaction and associated pH gradients in porewaters, Geochim. Cosmochim. Acta, 55, 145–159, 1991.
Boudreau, B. P.: Diagenetic models and their implementation: Modeling transport and reactions in aquatic sediments, Springer-Verlag, Heidelberg, 414 pp., 1997.
Boudreau, B. P.: Mathematics of tracer mixing in sediments. 1. Spatially-dependent, diffusive mixing, Am. J. Sci., 286, 161–198, 1986.
Borges, A. V.: Do we have enough pieces of the jigsaw to integrate CO_2 fluxes in the coastal ocean?, Estuaries, 28, 3–27, 2005.
Buscail, R., Pocklington, R., and Germain, C.: Seasonal variability of the organic-matter in a sedimentary coastal environment – sources, degradation and accumulation (continental-shelf of the Gulf-of-Lions, Northwestern Mediterranean-Sea), Cont. Shelf Res., 15, 843–869, 1995.
Canfield, D. E. and Berner, R. A.: Dissolution and pyritization of magnetite in anoxic marine sediments, Geochim. Cosmochim. Acta, 51, 645–659, 1987.
Canfield, D. E.: Sulfate reduction and oxic respiration in marine sediments: implications for organic carbon preservation in euxinic environments, Deep-Sea Res. Pt. I, 36, 121–138, 1989.
Canfield, D. E., Jorgensen, B. B., Fossing, H., Glud, R., Gundersen, J., Ramsing, N. B., Thamdrup, B., Hansen, J. W., Nielsen, L. P., and Hall, P. O.: J. Pathways of organic-carbon oxidation in three continental-margin sediments, Mar. Geol., 113, 27–40, 1993a.
Canfield, D. E., Thamdrup, B., and Hansen, J. W.: The anaerobic degradation of organic-matter in danish coastal sediments – iron reduction, manganese reduction, and sulfate reduction, Geochim. Cosmochim. Acta, 57, 3867–3883, 1993b.
Canfield, D. E.: Factors influencing organic carbon preservation in marine sediments, Chem. Geol., 114, 315–329, 1994.

Cathalot, C., Rabouille, C., Pastor, L., Deflandre, B., Viollier, E., Buscail, R., Grémare, A., Treignier, C., and Pruski, A.: Temporal variability of carbon recycling in coastal sediments influenced by rivers: assessing the impact of flood inputs in the Rhône River prodelta, Biogeosciences, 7, 1187–1205, doi:10.5194/bg-7-1187-2010, 2010.
Cathalot, C., Rabouille, C., Tisnerat-Laborde, N., Kerhervé, P., Bowles, K., Sun, M-Y., Tonczynski, J., Lansard, B., Treignier, C., Pastor, L.: Continental shelf particles: a major contributor of pre-aged organic carbon in deltaic areas, in preparation, 2011.
Chanton, J. P., Martens, C. S., and Goldhaber, M. B.: Biogeochemical cycling in an organic-rich coastal marine basin. 7. Sulfur mass balance, oxygen uptake and sulfide retention, Geochim. Cosmochim. Acta, 51, 1187–1199. 1987.
Charmasson, S., Bouisset, P., Radakovitch, O., Pruchon, A. S., and Arnaud, M.: Long-core profiles of Cs-137, Cs-134, Co-60 and Pb-210 in sediment near the Rhône River (Northwestern Mediterranean Sea), Estuaries, 21, 367–378, 1998.
Chen, C. T. A. and Borges, A. V.: Reconciling opposing views on carbon cycling in the coastal ocean: continental shelves as sinks and near-shore ecosystems as sources of atmospheric CO_2, Deep-Sea Res. Pt II, 56, 578–590, 2009.
Cline, J. D.: Spectrophotometric determination of hydrogen sulfide in natural waters, Limnol. Oceanog. 14, 454–458, 1969.
Copin-Montegut, C.: Alkalinity and carbon budgets in the Mediterranean Sea, Global Biogeochem. Cy., 7, 915–925, 1993.
Dedieu, K., Rabouille, C., Gilbert, F., Soetaert, K., Metzger, E., Simonucci, C., Jézéquel, D., Prévot, F., Anschutz, P., Hulth, S., Ogier, S., and Mesnage, V.: Coupling of carbon, nitrogen and oxygen cycles in sediments from a Mediterranean lagoon: a seasonal perspective, Mar. Ecol. Progr. Ser., 346, 45–59, 2007.
Deflandre, B., Mucci, A., Gagne, J. P., Guignard, C. and Sundby, B.: Early diagenetic processes in coastal marine sediments disturbed by a catastrophic sedimentation event, Geochim. Cosmochim. Acta, 66, 2547–2558, 2002.
De Madron, X. D., Abassi, A., Heussner, S., Monaco, A., Aloisi, J. C., Radakovitch, O., Giresse, P., Buscail, R., and Kerherve, P.: Particulate matter and organic carbon budgets for the gulf of lions (NW mediterranean), Oceanol. Acta, 23, 717–730, 2000.
Dhakar, S. P. and Burdige, D. J.: A coupled, non-linear, steadystate model for early diagenetic processes in pelagic sediments, Am. J. Sci., 296, 244–265, 1996.
Epping, E., van der Zee, C., Soetaert, K., and Helder, W.: On the oxidation and burial of

BGD
8, 549–592, 2011

Biogeochemical processes in the Rhône prodelta sediments

L. Pastor et al.

organic carbon in sediments of the Iberian Margin and Nazare Canyon (NE Atlantic), Progr. Oceanogr., 52, 399–431, 2002.

Gatti, J., Petrenko, A., Devenon, J.-L., Leredde, Y., and Ulses, C.: The Rhône river dilution zone present in the northeastern shelf of the Gulf of Lion in December 2003, Cont. Shelf Res., 26, 1794–1805, 2006.

García-García, A., Orange, D., Lorenson, T., Radakovitch, O., Tesi, T., Miserocchi, S., Berné, S., Friend, P. L., Nittrouer, C., and Normand, A.: Shallow gas off the Rhône prodelta, Gulf of Lions, Marine Geol., 234(1–4), 215–231, 2006.

Grasshoff, K., Ehrhardt, M., and Kremling, K.: Methods of Seawater Analysis, Verlag Chemie, Weinheim, 419 pp., 1983.

Haese, R. R., Schramm, J., van der Loeff, M. M. R., and Schulz, H. D.: A comparative study of iron and manganese diagenesis in continental slope and deep sea basin sediments off Uruguay (SW Atlantic), Int. J. Earth Sci., 88, 619–629, 2000.

Hall, P. O. and Aller, R. C.: Rapid, small-volume, flow injection analysis for ScO_2 and NH_4^+ in marine and freshwaters, Limnol. Oceanogr., 37, 1113–1119, 1992.

Hargrave, B. T. and Phillips, G. A.: Decay times of organic-carbon in sedimented detritus in a macrotidal estuary, Mar. Ecol.-Prog. Ser., 56, 271–279, 1989.

Hargrave, B. T., Holmer, M., and Newcombe, C. P.: Towards a classification of organic enrichment in marine sediments based on biogeochemical indicators, Mar. Pollut. Bull., 56(5), 810–824, 2008.

Hedges, J. I. and Keil, R. G.: Sedimentary organic matter preservation: an assessment and speculative synthesis, Mar. Chem., 49, 81–115, 1995.

Henrichs, S. M. and Reeburgh, W. S.: Anaerobic mineralization of marine sediment organic matter: rates and the role of anaerobic processes in the oceanic carbon economy, Geomicrobiology, 5, 191–236, 1987.

Helder, W.: Early diagenesis and sediment–water exchange in the Golfe du Lion. European Commission, Brussel, 1989.

Herman, P. M. J., Soetaert, K., Middelburg, J. J., Heip, C., Lohse, L., Epping, E., Helder, W., Antia, A. N., and Peinert, R.: The seafloor as the ultimate sediment trap-using sediment properties to constrain benthic-pelagic exchange processes at the goban spur, Deep-Sea Res. Pt. II, 48, 3245–3264, 2001.

Holligan, P. M. and Reiners, W. A.: Predicting the responses of the coastal zone to global change, Adv. Ecol. Res., 22, 211–255, 1992.

BGD
8, 549–592, 2011

Biogeochemical processes in the Rhône prodelta sediments

L. Pastor et al.

Huerta-Diaz, M. A. and Morse, J. W.: A quantitative method for determination of trace-metal concentrations in sedimentary pyrite, Mar. Chem., 29, 119–144, 1990.
Huerta-Diaz, M. A. and Morse, J. W.: Pyritization of trace metals in anoxic marine sediments, Geochim. Cosmochim. Acta, 56, 2681–2702, 1992.
Hulth, S., Tengberg, A., Landen, A., and Hall, P. O. J.: Mineralization and burial of organic carbon in sediments of the Southern Weddell Sea (Antarctica), Deep-Sea Res. Pt. I, 44, 955–981, 1997.
Ingall, E. and Jahnke, R.: Evidence for enhanced phosphorus regeneration from marine sediments overlain by oxygen depleted waters, Geochim. Cosmochim. Acta, 58, 2571–2575, 1994.
Jorgensen, B. B.: Sulfur cycle of a coastal marine sediment (Limfjorden, Denmark), Limnol. Oceanogr., 22, 814–832, 1977.
Jorgensen, B. B., Bang, M., and Blackburn, T. H.: Anaerobic mineralization in marine sediments from the Baltic Sea-North transition, Mar. Ecol. Progr. Ser., 59, 39–54, 1990.
Kasih, G. A. A., Chiba, S., Yamagata, Y., Shimizu, Y., and Haraguchi, K.: Numerical model on the material circulation for coastal sediment in Ago Bay, Japan, J. Mar. Syst., 77, 45–60, 2009.
King, G. M., Howes, B. L., and Dacey, J. W. H.: Short-term end-products of sulfate reduction in a salt marsh formation of acid volatile sulfides, elemental sulfur, and pyrite, Geochim. Cosmochim. Acta, 49, 1561–1566, 1985.
Kostka, J. E. and Luther, G. W.: Partitioning and speciation of solid phase iron in salt-marsh sediments, Geochim. Cosmochim. Acta, 58, 1701–1710, 1994.
Lansard, B., Rabouille, C., Denis, L., and Grenz, C.: In situ oxygen uptake rates by coastal sediments under the influence of the Rhône River (NW Mediterranean Sea). Symposium on Coastal Ecosystem Responses to Changing Nutrient Inputs from Large Temperate and Sub-Tropical Rivers, Fujian, China, 1501–1510, 2005.
Lansard, B., Rabouille, C., Denis, L., and Grenz, C.: Benthic remineralization at the land-ocean interface: a case study of the Rhône River (NW Mediterranean Sea), Estuar. Coast. Shelf Sci., 81, 544–554, 2009.
Littke, R., Baker, D. R., Leythaeuser, D., and Rullkötter, J.: Keys to the depositional history of the Posidonia Shale (Toarcian) in the Hils syncline, Northern Germany. Modern and Ancient Continental Shelf Anoxia, edited by: Tyson, R. V. and Pearson, T. H., Geol. Soc. London, Spec. Publ. 58, 311–334, 1991.

BGD
8, 549–592, 2011

Biogeochemical processes in the Rhône prodelta sediments

L. Pastor et al.

Lückge, A., Ercegovac, M., Strauss, H., and Littke, R.: Early diagenetic alteration of organic matter by sulfate reduction in Quaternary sediments from the Northeastern Arabian Sea, Mar. Geol., 158(1–4), 1–13, 1999.
Mackin, J. E. and Swider, K. T.: Organic matter decomposition pathways and oxygen consumption in coastal marine sediments, J. Mar. Res., 47, 681–716, 1989.
Maerki, M., Muller, B., Dinkel, C., and Wehrli, B.: Mineralization pathways in lake sediments with different oxygen and organic carbon supply, Limnol. Oceanogr., 54, 428–438, 2009.
Martens, C. S. and Val Klump, J.: Biogeochemical cycling in an organic-rich coastal marine basin 4. An organic carbon budget for sediments dominated by sulfate reduction and methanogenesis, Geochim. Cosmochim. Acta, 48, 1987–2004, 1984.
McKee, B. A., Aller, R. C., Allison, M. A., Bianchi, T. S. and Kineke, G. C.: Transport and transformation of dissolved and particulate materials on continental margins influenced by major rivers: benthic boundary layer and seabed processes, Cont. Shelf Res., 24, 899–926, 2004.
Miralles, J., Radakovitch, O., and Aloisi, J. C.: Pb-210 sedimentation rates from the northwestern mediterranean margin, Mar. Geol., 216, 155–167, 2005.
Monaco, A., de Madron, X. D., Radakovitch, O., Heussner, S., and Carbonne, J.: Origin and variability of downward biogeochemical fluxes on the Rhone continental margin (NW Mediterranean), Deep-Sea Res. Pt. I, 46, 1483–1511, 1999.
Mucci, A. and Morse, J. W.: The solubility of calcite in seawater solutions of various magnesium concentration, it=0.697 m at 25 °C and one atmosphere total pressure, Geochim. Cosmochim. Acta, 48, 815–822, 1984.
Pastor, L., Deflandre, B., Viollier, E., Cathalot, C., Metzger, E., Escoubeyrou, K., Lloret, E., Pruski, A., Buscail, R., Grémare, A., and Rabouille, C.: Influence of the organic matter composition on benthic oxygen demand in a deltaic system: The Rhône delta (NW Mediterranean Sea), Cont. Shelf Res., in revision, 2011.
Pedersen, T. F. and Price, N. B.: The geochemistry of manganese carbonate in panama basin sediments, Geochim. Cosmochim. Acta, 46, 59–68, 1982.
Pont, D., Simonnet, J. P., and Walter, A. V.: Medium-term changes in suspended sediment delivery to the ocean: Consequences of catchment heterogeneity and river management (Rhône River, France), Estuar. Coast. Shelf Sci., 54, 1–18, 2002.
Pratihary, A. K., Naqvi, S. W. A., Naik, H., Thorat, B. R., Narvenkar, G., Manjunatha, B. R., and Rao, V. P.: Benthic fluxes in a tropical Estuary and their role in the ecosystem, Estuar. Coast.

BGD
8, 549–592, 2011

Biogeochemical processes in the Rhône prodelta sediments

L. Pastor et al.

Shelf Sci., 85, 387–398, 2009.
Quintana, C. O., Tang, M., and Kristensen, E.: Simultaneous study of particle reworking, irrigation transport and reaction rates in sediment bioturbated by the polychaetes heteromastus and marenzelleria, J. Exp. Mar. Biol. Ecol., 352, 392–406, 2007.
Rabouille, C. and Gaillard, J. F.: Toward the EDGE: Early diagenetic global explanation: A model depicting the early diagenesis of organic matter, O_2, NO_3, Mn, and PO_4, Geochim. Cosmochim. Acta, 55, 2511–2525, 1991.
Radakovitch, O., Charmasson, S., Arnaud, M., and Bouisset, P.: Pb-210 and caesium accumulation in the Rhône delta sediments, Estuar. Coast. Shelf Sci., 48, 77–92, 1999.
Raiswell, R., Canfield, D. E., and Berner, R. A.: A comparison of iron extraction methods for the determination of degree of pyritisation and the recognition of iron-limited pyrite formation, Chem. Geol., 111, 101–110, 1994.
Rasmussen, H. and Jorgensen, B. B.: Microelectrode studies of seasonal oxygen uptake in a coastal sediment: role of molecular diffusion, Mar. Ecol. Prog.-Ser., 81, 289–303, 1992.
Revsbech, N. P.: An oxygen microsensor with a guard cathode, Limnol. Oceanogr., 34, 474–478, 1989.
Rhoads, D. C. and Cande, S.: Sediment profile camera for in situ study of organism-sediment relations, Limnol. Oceanogr., 16, 110–114, 1971.
Rizzo, W. M. and Christian, R. R.: Significance of subtidal sediments to heterotrophically-mediated oxygen and nutrient dynamics in a temperate estuary, Estuaries, 19, 475–487, 1996.
Rysgaard, S., Thamdrup, B., Risgaard-Petersen, N., Fossing, H., Berg, P., Christensen, P. B., and Dalsgaard, T.: Seasonal carbon and nutrient mineralization in a high-arctic coastal marine sediment, young sound, Northeast Greenland, Mar. Ecol.-Prog. Ser., 175, 261–276, 1998.
Sempere, R., Charriere, B., Van Wambeke, F., and Cauwet, G.: Carbon inputs of the Rhone River to the Mediterranean Sea: biogeochemical implications, Global Biogeochem. Cy., 14, 669–681, 2000.
Soetaert, K., Herman, P. M. J., and Middelburg, J. J.: A model of early diagenetic processes from the shelf to abyssal depths, Geochim. Cosmochim. Acta, 60, 1019–1040, 1996a.
Soetaert, K., Herman, P. M. J., and Middelburg, J. J.: Dynamic response of deep-sea sedimentsto seasonal variations: a model, Limnol. Oceanogr., 41, 1651–1668, 1996b.
Soetaert, K., Herman, P. M. J., Middelburg, J. J., and Heip, C.: Assessing organic matter

Discussion Paper | Discussion Paper | Discussion Paper | Discussion Paper |

mineralization rate, degradability and mixing rate in an ocean margin sediment (North-East Atlantic) by diagenetic modelling, J. Mar. Res., 56, 519–534, 1998.
Soetaert, K. and Herman, P. M. J.: "A practical guide to ecological modelling – using R as a simulation platform", Springer Science + Business Media, B.V., 372 pp., 2009.
Soetaert, K., Petzoldt, T., and Meysman, F.: marelac: Tools for Aquatic Sciences. R package version 2.1, available at: http://cran.r-project.org/web/packages/marelac, 2010.
Tabatabai, M. A.: A rapid method for determination of sulfate in water samples, Environ. Lett., 7(3), 237–243, 1974.
Tesi, T., Miserocchi, S., Goni, M. A., and Langone, L.: Source, transport and fate of terrestrial organic carbon on the Western Mediterranean Sea, Gulf of Lions, France, Mar. Chem., 105, 101–117, 2007.
Thamdrup, B. and Dalsgaard, T.: The fate of ammonium in anoxic manganese oxide-rich marine sediment, Geochim. Cosmochim. Acta, 64(24), 4157–4164, 2000.
Thamdrup, B., Fossing, H., and Jorgensen, B. B.: Manganese, iron and sulfur cycling in a coastal marine sediment, Aarhus Bay, Denmark, Geochim. Cosmochim. Acta, 58, 5115–5129, 1994.
Thomsen, U., Thamdrup, B., Stahl, D. A., and Canfield, D. E.: Pathways of organic carbon oxidation in a deep lacustrine sediment, Lake Michigan, Limnol. Oceanogr., 49, 2046–2057, 2004.
Tromp, T. K., Van Cappellen, P., and Key, R. M.: A global model for the early diagenesis of organic carbon and organic phosphorus in marine sediments, Geochim. Cosmochim. Acta, 59(7), 1259–1284, 1995.
Van Cappellen, P. and Wang, Y.: Cycling of iron and manganese in surface sediments: a general theory for the coupled transport and reaction of carbon, oxygen, nitrogen, sulfur, iron, and manganese, Am. J. Sci., 296, 197–243, 1996.
Wakeham, S. G., Lee, C., Hedges, J. I., Hernes, P. J., and Peterson, M. L.: Molecular indicators of diagenetic status in marine organic matter, Geochim. Cosmochim. Acta, 61(24), 5363–5369, 1997.
Wang, Y. and Van Capellen, P.: A multicomponent reactive transport model of early diagenesis: application to redox cycling in coastal sediments, Geochim. Cosmochim. Acta, 60, 2993–3014, 1996.
Westrich, J. T. and Berner, R. A.: The role of sedimentary organic matter in bacterial sulfate reduction – the g model tested, Limnol. Oceanogr., 29, 236–249, 1984.

Wijsman, J. W. M., Herman, P. M. J., Middelburg, J. J., and Soetaert, K.: A model for early diagenetic processes in sediments of the continental shelf of the Black Sea, Estuar. Coast. Shelf Sci., 54, 403–421, 2002.

Wollast, R.: Evaluation and comparison of the global carnon cycle in the coastal zone and in the open ocean, in: The Sea, the Global Coastal Ocean, Processes and Methods, edited by: Brink, K. H. and Robinson, A. R., Wiley and Sons, New York, 213–252, 1998.

Zuo, Z., Eisma, D., Gieles, R., and Beks, J.: Accumulation rates and sediment deposition in the North-Western Mediterranean, Deep-Sea Res. Part II, 44, 597–609, 1997.

Zuo, Z., Eisma, D., and Berger, G. W.: Determination of sediment accumulation and mixing rates in the Gulf of Lions, Mediterranean Sea, Oceanol. Acta, 14, 253–262, 1991.

BGD

8, 549–592, 2011

Biogeochemical processes in the Rhône prodelta sediments

L. Pastor et al.

Table 1. Sampling sites location together with sediment oxygen consumption fluxes (TOU), ammonium and nitrate release to the bottom water measured from core incubation and compared to values estimated by the model; All fluxes are expressed in mmol m^{-2} d^{-1}.

Sites	Lat. (° N)	Long. (° E)	Depth (m)	Dist (km)	TOU data	DOU data	DOU model	NH_4^+ data	NH_4^+ model	NO_3^- data	NO_3^- model
A	43°18′8	4°51′1	24	1.9	15.6 ± 5.0	21.5 ± 3.9	26.4	4.92 ± 2.89	2.56	–	3.94
B	43°18′2	4°50′1	57	3	15.9 ± 3.6	15.7 ± 2.1	18.1	0.63 ± 0.49	0.95	0.24 ± 0.07	0.60
K	43°18′1	4°51′5	62	3.3	10.2 ± 2.2	10.8 ± 2.2	12.1	0.32 ± 0.16	0.45	0.21 ± 0.09	1.02
L	43°18′3	4°52′9	61	4	11.8 ± 9.8	7.0 ± 3.9	10.4	2.01 ± 1.91	0.28	0.32 ± 0.12	0.90
N	43°17′5	4°48′0	65	5.5	11.4 ± 2.6	9.5 ± 1.2	13.9	–	0.65	0.41 ± 0.17	0.68
I	43°16′0	4°53′0	89	7.7	10.1 ± 0.9	4.6 ± 0.8	7.3	–	0.42	0.12 ± 0.08	0.31
C	43°16′3	4°46′6	76	8.6	7.8 ± 0.6	10.3 ± 3.2	13.2	0.24 ± 1.29	0.20	0.37 ± 0.08	1.20
J	43°16′1	4°58′1	86	12.1	9.6 ± 2.0	7.2 ± 3.3	8.6	–	0.09	0.27 ± 0.09	0.84
F	43°10′0	4°42′0	78	21.6	7.0 ± 2.0	5.3 ± 0.7	6.7	–	0.07	–	0.55

– no data. Standard deviations are determined from 2 or 3 cores.

BGD

8, 549–592, 2011

Biogeochemical processes in the Rhône prodelta sediments

L. Pastor et al.

Table 2. Adjusted parameters.

Sites	A	B	K	L	N	I	C	J	F
Fdeg (g C/m^2/yr)	657	107	88	70	101	42	71	52	32
Pfast (%)	50	80	60	80	50	90	94	75	80
Rfast (/yr)	11	33	33	33	33	33	33	33	33
Rslow (/yr)	0.31	0.29	0.31	0.32	0.37	0.37	0.21	0.36	0.33
Asymptotic OC (%)	2.5	1.7	1.3	1.2	1.2	0.93	1	0.95	0.9
biot (cm^2/yr)	1	1	3	3	3	10	5	10	10
ODUdepo (%)	99.5	97.4	98.7	97.0	99.2	97.6	98.0	97.0	97.6
Rnit (/d)	100	20	80	50	16	4	100	100	23

Fdeg, Degradable organic carbon flux; Pfast, proportion of fast OM; Rfast and Rslow, first order decay rates for the fast and slow fraction of OM, respectively; Asymptotic OC, organic content at the bottom of the core; biot, bioturbation rate; ODUdepo, ODUs precipitation coefficient; and Rnit, nitrification rate.

BGD

8, 549–592, 2011

Biogeochemical processes in the Rhône prodelta sediments

L. Pastor et al.

Table 3. Degradation rates of organic carbon by oxic mineralization, denitrification and anoxic mineralization (in $mmol\,C\,m^{-2}\,d^{-1}$) and the relative contribution to the oxygen consumption by oxic mineralization, nitrification and ODUs reoxidation (in %).

Sites	Organic carbon degradation processes ($mmol\,C\,m^{-2}\,d^{-1}$)			Relative use of oxygen (%)		
	Oxic mineralization	Denitrification	Anoxic mineralization	Oxic mineralization	Nitrification	ODU reoxidation
A	12.0	4.0	134.0	62.2	36.9	1.0
B	15.7	0.7	8.2	92.3	6.7	1.0
K	9.2	0.5	10.3	85.9	13.0	1.2
L	7.1	0.8	8.1	80.5	17.1	2.4
N	11.6	0.6	10.8	90.5	8.8	0.6
I	6.4	0.1	3.1	92.9	6.0	1.1
C	9.4	0.9	5.9	82.5	16.6	0.9
J	5.7	0.6	5.4	79.3	18.6	2.1
F	4.9	0.4	2.0	84.7	14.4	0.8

BGD
8, 549–592, 2011

Table 4. Carbon mineralization rates as calculated from (1) modeling and (2) in situ oxygen microprofiling. Units are $g\,C\,m^{-2}\,yr^{-1}$.

Sites	Carbon mineralization from modeling	Carbon mineralization from oxygen profiles
A	657	72 ± 13
B	107	53 ± 7
K	88	36 ± 7
L	70	24 ± 13
N	101	32 ± 4
I	42	15 ± 3
C	71	35 ± 11
J	52	24 ± 11
F	32	18 ± 2

BGD
8, 549–592, 2011

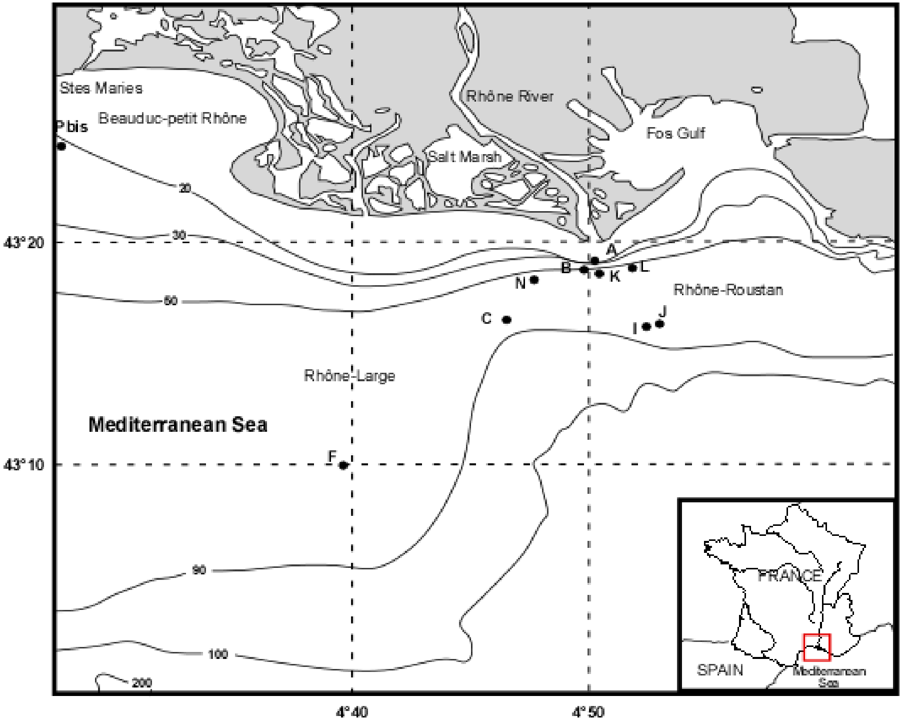

Fig. 1. Sampling sites in the close vicinity of the Rhône River mouth.

BGD
8, 549–592, 2011

Biogeochemical processes in the Rhône prodelta sediments

L. Pastor et al.

Title Page
Abstract Introduction
Conclusions References
Tables Figures
◀I ▶I
◀ ▶
Back Close
Full Screen / Esc
Printer-friendly Version
Interactive Discussion

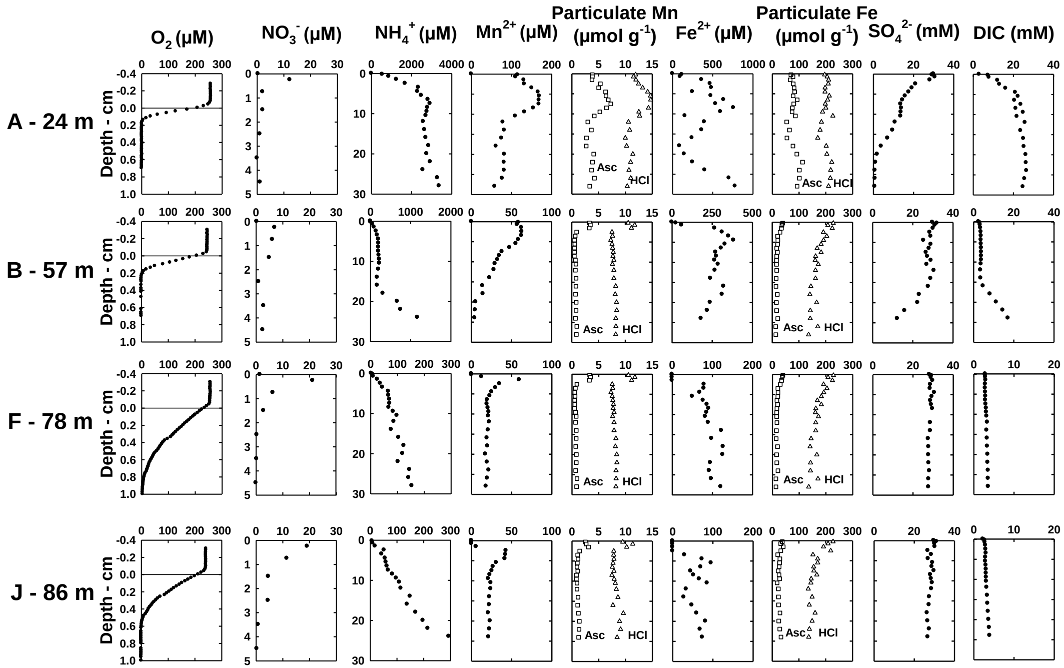

Fig. 2. Biogeochemical profiles in sediments from stations A, B, F and J: mean oxygen, nitrate, ammonium, dissolved manganese and iron, particulate manganese and iron extracted with HCl and an ascorbate solution, sulphate and DIC. Note that different scales are used for different stations.

BGD
8, 549–592, 2011

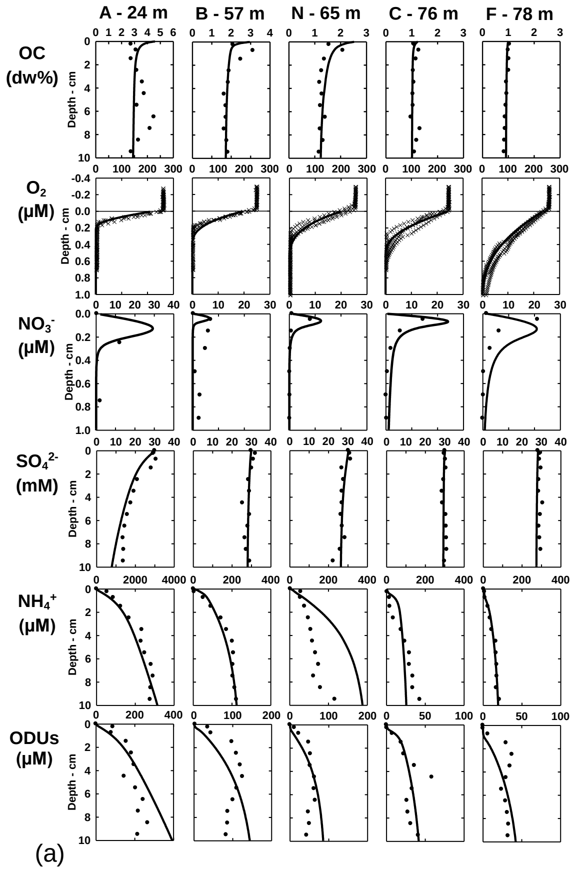

Fig. 3. Experimental profiles (symbols) and the best fit using the steady-state version of OMEX-DIA, a numerical coupled diagenetic model (lines) **(a)** in sites A, B, N, C and F and **(b)** in sites K, L, I and J. Note that different scales are used for different stations.

BGD

8, 549–592, 2011

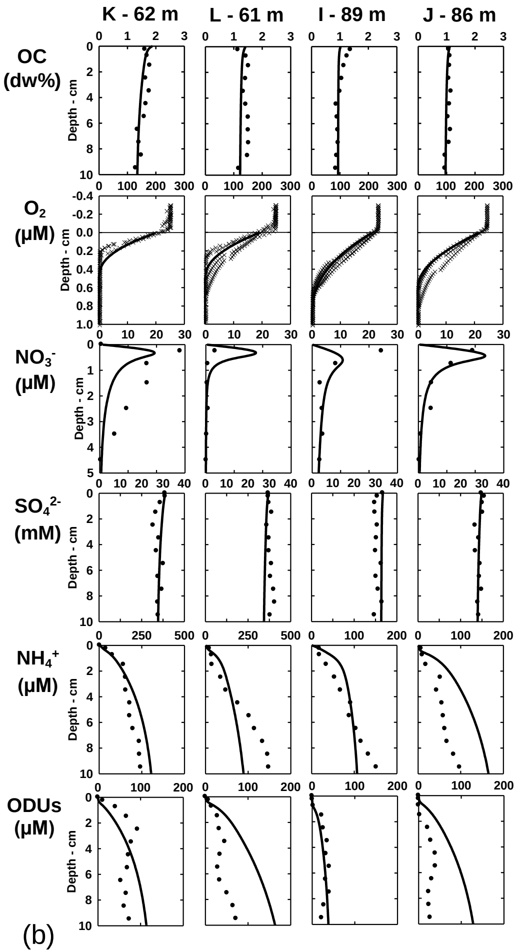

Fig. 3. Continued.

BGD

8, 549–592, 2011

Biogeochemical processes in the Rhône prodelta sediments

L. Pastor et al.

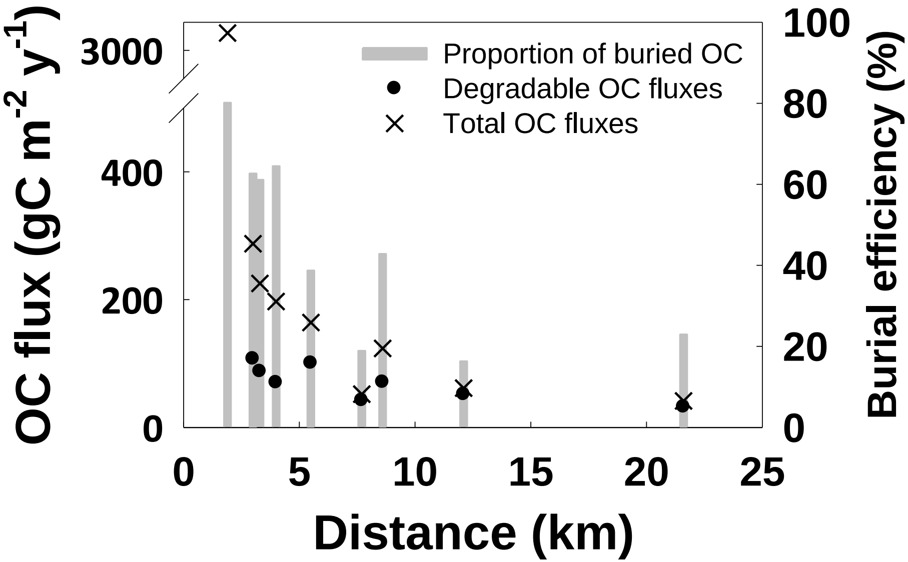

Fig. 4. Flux of degraded • and total × organic carbon (OC) together with burial efficiency as a function of distance from the Rhône River outlet.

BGD
8, 549–592, 2011

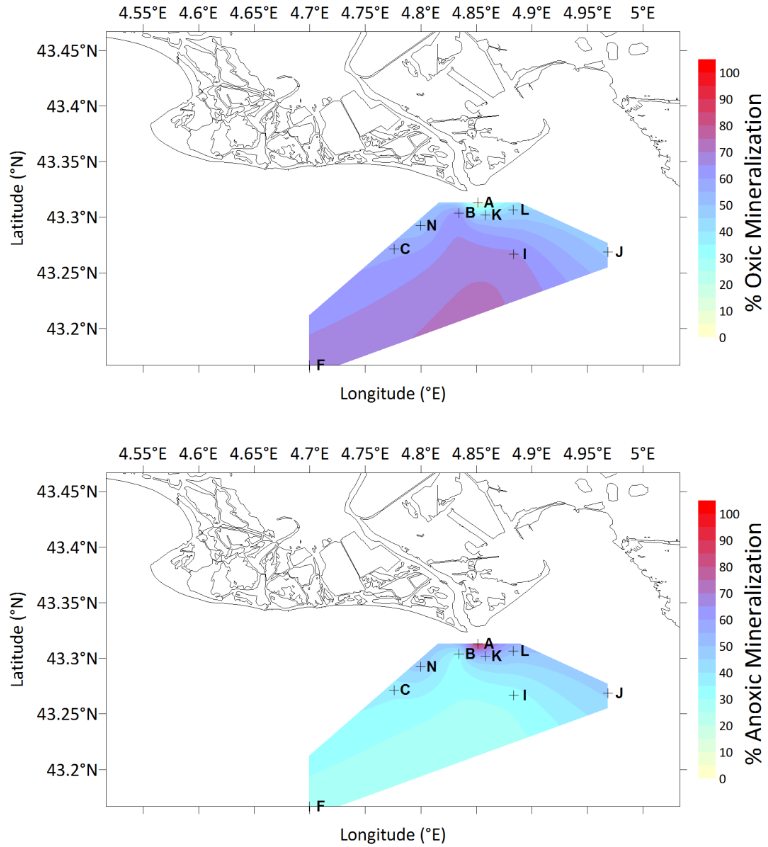

Fig. 5. Relative contribution of principal organic carbon mineralization pathways (oxic mineralization and anoxic mineralization) on total organic carbon mineralization expressed in % in the Rhône River prodelta and its adjacent continental shelf. Denitrification process accounted for less than 6%.

BGD

8, 549–592, 2011

Biogeochemical processes in the Rhône prodelta sediments

L. Pastor et al.

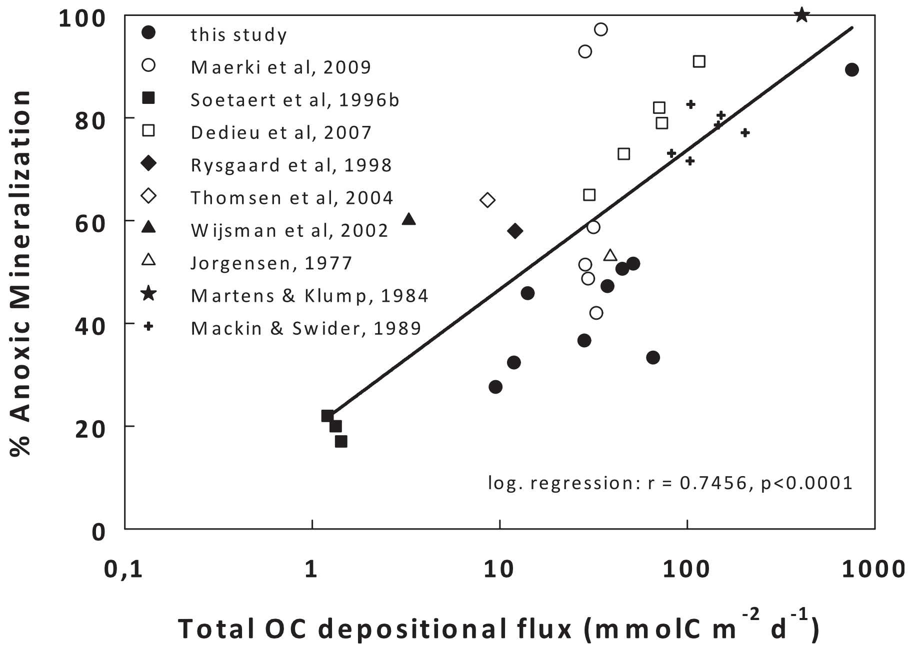

Fig. 6. Contribution of anoxic processes in total OC mineralization as a function of total OC depositional flux for the Rhône River prodelta and its adjacent continental shelf (this study) and a compilation of several data.

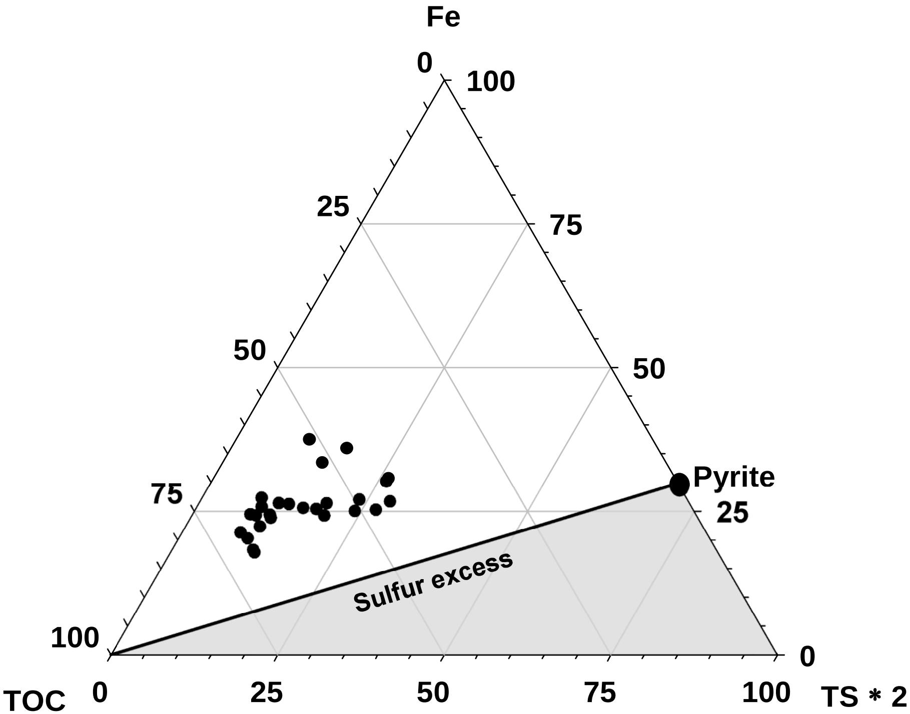

Fig. 7. Ternary plot of carbon-iron-sulfur relationship. The shaded area represents the field of iron limitation. Sulfur was multiplied by 2 (2 moles of C produce 1 mole of S). Iron was determined from solid extraction with HCl. Data are from stations A and K.

BGD

8, 549–592, 2011

Biogeochemical processes in the Rhône prodelta sediments

L. Pastor et al.